MICHIGAN STATE UNIVERSITY

CYCLOTRON LABORATORY

SUPERCONDUCTING CYCLOTRONS FOR HEAVY IONS

F. G. RESMINI

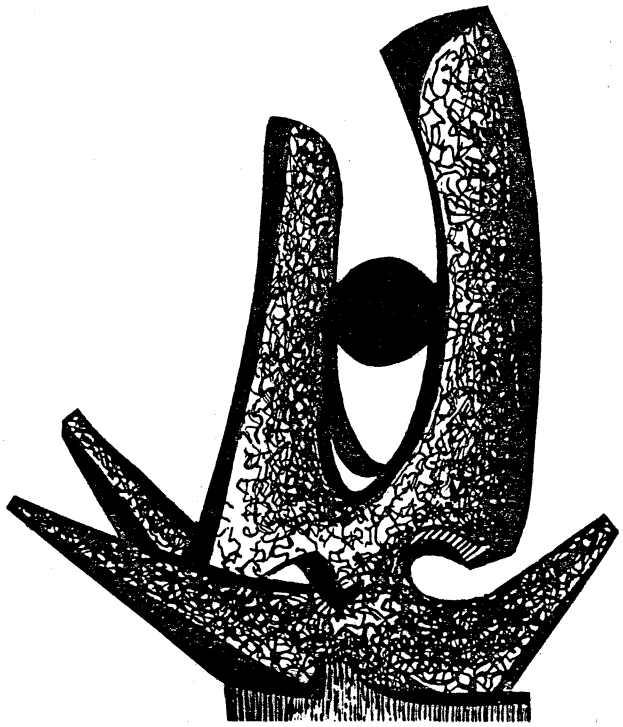

OCTOBER 1980

MSUCL-341

MSUCL-341
October 1980

SUPERCONDUCTING CYCLOTRONS FOR HEAVY IONS[+]

F.G. Resmini[+]-Michigan State University, East Lansing, Michigan

1. Introduction

Even though no superconducting cyclotron is yet in operation, it appears that these machines will play, in the coming years, a substantial role in the rapidly developing field of heavy ion acceleration. In fact, in the energy domain up to a few hundred MeV/nucleon, superconducting cyclotrons seem to offer definite advantages in terms of size, energy variability and overall flexibility (internal or external ion sources both look possible), when compared with more conventional options like room temperature cyclotrons and linacs. The admittedly higher construction complexity, which partially derives from the intrinsic novelty of these machines, is more than offset by the large cost savings that are made possible by the superconducting magnets technology.

It is the purpose of this paper to briefly review the current state of heavy ion acceleration and to illustrate some of the main features of these machines. Their possible relevance in connection with the general purposes of the "MARIA" project is also discussed.

2. Present status of large ion accelerators

In order to put in a proper perspective the rapid development which is characteristic of heavy ion acceleration, Figure 1 presents in the customary T/A vs A diagram the major facilities now operating in the world. It is noted that a substantial range of energies, roughly between 50 and several hundreds MeV/n is not accessible.

[+] Prepared for the "MARIA" Workshop - University of Alberta, Edmonton, Canada, October 20-24, 1980.

It is precisely with the goal of filling this gap that several accelerators are now in construction around the world, as shown in Figure 2. The type of machines involved in this large scale effort are schematically presented in Figure 3. Superconducting cyclotrons are present in the Chalk River project, as a K=520 booster to a 13 MeV tandem, in the MSU Phase I, which entails the use of an internal ion source, for a K=500 cyclotron; and in the MSU Phase II, where a K=800 cyclotron is used as booster for the previous one. The Oak Ridge project involves a 25 MeV tandem which injects into a conventional K100 cyclotron (ORIC), while GANIL consists of two room temperature K=400 separated sector cyclotrons, coupled together.

The interest in heavy ion physics has meanwhile prompted a number of other proposals from quite a few laboratories around the world. Their goals in terms of energy per nucleon vs A are presented in Figure 4. Although it is likely that only a few of these will eventually be built, it is clear that a large research and development effort is to be expected in this field in the next few years.

Even though it is outside the scope of this paper to enter into the details of the various proposals, superconducting cyclotrons are envisaged, one way or another, in a number of them, reflecting an increasing confidence in this newly developing technology.

3. Superconducting cyclotrons: Theoretical considerations

3.1 General remarks

As well known, a superconducting cyclotron is basically like an ordinary A.V.F. cyclotron, with iron sectors providing the necessary field modulation for the axial focusing, while the

average magnetic field must increase with radius so as to fulfill the isochronism. However, the use of superconducting costs allows one to obtain average magnetic fields in the range of 25 to 50 kgauss, i.e. well in excess of those (18 kgauss at most) encountered in conventional cyclotrons. At these field values, the iron of the pole tips is completely saturated, a condition which has some consequences worth discussing in detail.

As in ordinary cyclotrons we can write the magnetic field as a function of the radius R and azimuth

$$\theta \text{ as } B(R,O)=\bar{B}(R)+\sum_{n=1} C_n(R) \cos (n\theta+\Phi_n(R)) \qquad (1)$$

Ordinarily only the harmonics of order N, 2N, 3N etc., where N is the number of sectors, will have any significant value.

The average field, $\bar{B}(R)$ must satisfy the isochronism condition, i.e.

$$\omega = \frac{e\,\bar{B}(R=o)}{A\,m_o} = \frac{Z}{A}\,\frac{e\,\bar{B}(R)}{m} = \text{const} \qquad (2)$$

Z and A being the charge state and mass number of the accelerated ion. Writing $B_o = \bar{B}(R=O)$ the isochronism condition obviously implies that $\bar{B}(R)=B_o/\sqrt{1-\beta^2}$ or , as a function of radius:

$$\bar{B}(R) \simeq \frac{B_o}{\sqrt{1-\frac{\omega^2}{c^2}R^2}} \qquad (3)$$

The radial and axial focusing frequencies, in the customary ν_R and ν_Z notation, can be expressed, as in conventional cyclotrons by:

$$\nu_R^2 \simeq 1+k+ \text{ higher order terms} \qquad (4)$$

$$\nu_Z^2 \simeq -k+F(1+2\,tg^2\gamma) + \text{higher order terms} \qquad (5)$$

where:

k is the field index $= \frac{R}{\bar{B}(R)}\,\frac{d\bar{B}(R)}{dR} = \frac{\beta^2}{1-\beta^2} = \frac{E}{E_o}^2 - 1$

F is the flutter $= \sum_{M=1}^{\infty} \frac{1}{2}\,\frac{C_n^2}{\bar{B}^2}$ and

γ is the usual angle between the tangent to the sector spiral and the radius. Refering to the previous notation, $tg\,\gamma = R\,\frac{d\phi}{dR^n}$, or, for a spiral sector following a law of the type $\theta = \alpha R$ with α constant, $tg\,\gamma = \alpha R$.

The first and most important consequence of the iron saturation is that the field modulation, i.e. the C_n amplitudes in (1) remain constant over the entire range of average magnetic fields. This in turn implies that the flutter F varies as $\frac{1}{\bar{B}^2}$, and therefore decreases the higher the average field. It can be proven in a straight forward way from eq(5) that in order to have axial focusing, i.e. $\nu_Z^2 > 0$, it must be

$$\frac{T}{A} \underset{\text{MeV/n}}{\leq} K_{Foc}\left(\frac{Z}{A}\right) \qquad (6)$$

where (T/A), kinetic energy/nucleon is usually expressed in MeV/n, and K_{Foc} is proportional to C_N, R, and Tg γ. This equation together with the customary bending condition, i.e.

$$\frac{T}{A} \underset{\text{MeV/n}}{\leq} K\left(\frac{Z}{A}\right)^2 \qquad (7)$$

where K is proportional to $\bar{B}^2 R^2$, defines the operating range, in terms of energy/nucleon, of a superconducting cyclotron.

As an order of magnitude example, a K 800corresponds to an extraction radius of about 90cm and a field, at extraction, of 49 kgauss. Typically it is found that K_{Foc} can assume, for any

given machine, a maximum value not exceeding approximately 1/3 of the corresponding maximum K value, if the latter is calculated for the given extraction radius and a field value around 49-50 kgauss. For example, the MSU K=500 cyclotron has a K_{Foc} = 160, while the second stage, which can reach K=1200, has a K_{Foc}=400. The Chalk River K 500 cyclotron also has a K_{Foc} 110.

Therefore the cross-over between equations (6) and (7), or in other words K_{Foc} and K, in determining the maximum energy available for a given ion occurs typically at values of A/Z ≃.3 or less. For Z/A values higher than that the energy is determined by ex(6), and by ex(7) for lower Z/A.

3.2 Resonance limits

As in A.V.F. conventional cyclotrons, superconducting cyclotrons do have operating limits set by the presence of resonances. For the present purposes,it is sufficient to discuss only two of these resonances, i.e.:

$$\nu_R, \nu_Z = \frac{N}{2} \qquad (8)$$

$$\nu_R + 2\nu_Z = N \qquad (9)$$

which actually have a precise impact on the cyclotron performance Other resonances, like the $\nu_R = 1$ or $\nu_R = 2\nu_Z$, are of course also present, but their effect is very much the same as in conventional cyclotrons.

The first type, eq(8) corresponds to the existence of stopbands in the radial (axial) motion and, as in conventional cyclotrons, sets a limit on the maximum energy achievable with a given machine. For example,for N=3 ν_R or ν_Z must be less than 1.5, since the stopband cannot be crossed. In a three sector machine like the MSU

K800, for a 200 MeV/n beam ν_R reaches a maximum value of ≃1.38, which is higher than one would estimate from eq(4) due to the effect of higher order terms. As a consequence, an energy of about 220-240 MeV/n is the absolute maximum which could be reached with a three sector cyclotron. In order to go higher one must use a four sector geometry where, according to calculations, the ν_R = 4/2 = 2 limit would be reached between 380 and 400 MeV/n. Still higher energies would of course be reached, in principle, with six sectors, but the practicality of such a scheme in a high field compact machine is very questionable.

The second type, eq (9) is a coupling resonance between the radial and axial motion, which is intrinsic in the sense that it does not depend upon imperfections present in the magnetic field. It cannot be crossed, in general, unless the beam is perfectly centered, a condition which is very hard to meet,or else the beam literally "jumps" over the resonance. The latter condition corresponds to a very high energy gain/turn, which is unlikely to be met in most instances. Physically, the presence of this resonance in superconducting cyclotrons is generated by the increase of the flutter F at low magnetic fields, according to the $1/\bar{B}^2$ law explained above. This in turn increases strongly the value of ν_Z, a fact not usually observed in conventional cyclotrons where the iron is non-saturated, and generates therefore the conditions, according to eq(9), for the appearance of the resonance. As a consequence, as will be seen shortly, the resonance usually poses a limit on the lowest operational field, and tends therefore to restrict the dynamic range of a given machine. Again, there will be an advantage, from this point of view, in going from a three

sector to a four sector geometry.

4. The MSU superconducting cyclotrons

In order to illustrate some of the points emerging from the previous discussion, we shall mostly refer to the MSU superconducting cyclotron program, where construction of the K=500 is near completion, while the K=800 has just been started. For the sake of clarity the main parameters of both machines are listed in Table I, while main coil parameters are listed in Table II. More details can be found in ref. 1 to 7.

As is well known,the K=500 will initially operate as a stand alone machine, with an internal ion source of the PIG type. In this case it will have a T/A vs A operating diagram as shown in Fig. 5, the energies obviously depending upon the charge states delivered by the ion source. Upon completion of the K-800 cyclotron, the K=500 will be used mostly as injector to the latter, with beams injected into the median plane and stripped at an appropriate radius inside the K=800. Such a scheme is outlined in Fig. 6 and in more detail, for 200 MeV/n beams, in Fig. 7. The corresponding T/A vs A diagram for the K=800 cyclotron is shown in Fig. 8, together with the lines corresponding to constant charge states of beams delivered from the K=500 cyclotron. More details on the injection and coupling of the two cyclotrons can be found in (2,3). The accelerating voltage frequency of both machines spans the same range of 9 to 32 MHz, since the coupling is done at exactly the same frequency for any given ion. For the K=500 cyclotron the diagram of the energy vs R.F. frequency is presented, for a few harmonic modes, in Fig. 9, and for the two machines coupled together in Fig. 10. Note that, when used as

TABLE I. MAIN ACCELERATOR PARAMETERS

PARAMETER	K=500	K=800
Maximum K	500	1200
K_{Foc}	160	400
Max energy(Z/A=.5 ions)	80 MeV/n	200 MeV/n
Pole radius	25.75"	42"
N° of sectors	3, 46° wide	3,46° wide
Minimum hill gap	2.5"	3"
Max. valley gap	36"	36"
Spiral constant (approx)	1/13 rad/inch	1/13 rad/inch
Minimum-max operating fields	30-50 kgauss	30-50 kgauss
Yoke height	86"	117"
Yoke inner-outer diameters	84"-120"	118"-174"
R.F. frequency range	9-32 MHz	9-32 MHz
Harmonic operating modes	1st,2nd,3rd,4th	1st,2nd
Peak dee voltage	100 kV	200 kV
R.F. power per dee	$\leq$50 kW	$\leq$150 kW
No of trim coils	13	22
Max operating trim coil current	400 A	400 A
Max total trim coil power	50 kW	70 kW
Ion source	internal	internal and stripping of K=500 beams

TABLE II. COIL PARAMETERS

PARAMETER	K=500	K=800
Inner coil radius	30"	45.5"
Outer coil radius	35.5"	51.5"
Total coil height	19.25"	26.5"
Coil splitting	Two sections	Two sections
Height of sect. closer to med. plane	6.41"	16"
Minimum coil distance from med. plane	1.5"	2"
Max average current density	3500 A/cm^2	3500 A/cm^2
Nominal Max current	700 A	1000 A
Ampere turns at max current	4.8 10^6	7.2 10^6

injector, the K=500 will only have to deliver beams in the range of .5 to 7-8 MeV/n.

Perhaps the best way to summarize the performance of a superconducting cyclotron relative to the limits discussed earlier is to look at its operating diagram in a (B_o, Z/A) plane. This is done, for the K=500 cyclotron, in Fig. 11 where the boundaries of the diagram (bending limit, powering limit) are indicated together with constant energy per nucleon lines. The low field limit, arising from the $\nu_R + 2\nu_2 = 3$ resonance, is about 30 kgauss for this machine. An analogous diagram, for the K=800, is presented in Fig. 12 and with constant energy/nucleon lines, in Fig. 13. Again, the low field limit posed by the resonance is around 30 kgauss, for Z/A=.5 ions, and somewhat higher, 35 kgauss, for very small Z/A. The operating diagram of the K=500 cyclotron when acting as an injector is shown

in Fig. 14. Note that this diagram only shows, as said earlier, energies up to 7-8 MeV/n and a rather small Z/A range, in agreement with the low charge states as required in Fig. 8.

The examination of these operating diagrams also show that a superconducting cyclotron of the kind described here is not appropriate for accelerating protons. It is obvious, in fact, that in order to accelerate protons one should drop to rather low field values, like 18 or 20 kgauss, and the beam would hit the $\nu_R + 2\nu_2 = 3$ resonance well before the extraction radius. Also the trimming requirements for the magnetic field would be enourmously different from those for heavy ions implying very large and probably non realistic trim coil powers. At the present stage it looks then like the only reasonable way of getting protons is to accelerate molecular hydrogen Z/A = .5, and strip it to protons after extraction.

It would exceed the scope of this paper to go much into construction details of superconducting cyclotrons, also because rather precise descriptions of the projects now underway are published elsewhere.[1,3,8] However it is perhaps worth pointing out briefly the main aspects which make them very different from conventional cyclotons:

-Yokes are closed, with cylindrical shapes as in the MSU cyclotrons, or octagonal as in the Chalk River project, [8] for the purpose both of reducing the iron weight and minimizing the outer fringing field.

- The main coils are split into two sections, independently excited. The reason for it, as can be appreciated from Fig. 15, which refers to the K=500 cyclotron, is that the section closer to the median plane has a very different air core field from

the one farther away. Since the shape of the iron produced field, at saturation, is very much constant, the combination of the air core fields allows one to obtain easily the required field isochronism for different ions, therefore minimizing the requirements for trim coil powers. This gives rise to the peculiar operating diagram shown, again for the K=500, in Fig. 16. The fractional splitting of the main coils is usually optimized depending upon the maximum and minimum energy of the accelerated ions. (For example in the K=800 cyclotron, the section closer to the median plane is 0.6 of the total coil height). Examples of isochronous fields thus obtained for the K=500 cyclotron and Z/A = .5 ions are shown in Fig. 17.

- Given the very small hill gap (See Table I), the dees must be in the valleys. Also, since access to the median plane is limited by the main coils, which are as close to it as practical, the dees are driven by coaxial $\lambda/4$ lives inserted through the poles and the yoke.

- Extraction is accomplished by means of electrostatic deflectors and magnetic channels, as shown schematically in Fig. 18 for the K=500 cyclotron. The electrostatic deflectors run at most at 130-140 kV/cm. The magnetic channels used in the K=500 are of the passive type and provide radially focusing gradients as shown in Fig. 19. The main difference with respect to conventional cyclotrons is that the extraction path is typically much longer, i.e. of about 300^{o} - 320^{o}. An active magnetic channel is used in Chalk River [8] instead of the passive one, but the main extraction features are unchanged.

- Final trimming of the magnetic field is done either with trim coils, as at MSU, where they are wound around the hills,

or with movable trim rods as in Chalk River. [8] The choice between the two systems is mostly a matter of designer's choice, since both yield excellent results in terms of the desired magnetic field trimming.

5. Relevance of superconducting cyclotrons to the "MARIA" project.

Even though, from the preceding discussion, the superconducting cyclotron comes across as a very versatile, compact, and high performance heavy ion accelerator, it does not seem, as of now, to be an appropriate choice in light of the more recent "MARIA" requirements, which call for heavy ion beams of up to 1 GeV/n. We shall discuss separately the possibilities of a cyclotron as a single stage machine, or as injector.

5.1. Single stage cyclotron

Given the limitations discussed in sect. 3 and 4, a single stage superconducting cyclotron could, at present day, accelerate Z/A = .5 ions only up to $\simeq$400 MeV/n. As stated earlier higher energies would require at least six sectors and probably unrealistic pole dimensions. For a maximum energy of $\simeq$400 MeV/n the machine could have a pole diameter of 4.4 meters and would operate with a central field of 21 Kgauss, rising to 29.6 kgauss at extraction. The four sectors should have a spiral constant of at least 1/24 or 1/23 rad/inch. These data are obviously tentative, and are derived from an extrapolation of known K=800 data.

In view of present "MARIA" goals a machine of this kind cannot now be proposed. However, should limited depth therapy be considered, in the future, as a first necessary exploratory stage, such a cyclotron could be considered more seriously, given its relative low cost. In conjunction with axial injection from sources

like the EBIS or ECR types, which can provide fully stripped light ion beams, such a single stage facility could be rather attractive. Obviously at that point a serious design study should be undertaken to verify whether and how such a cyclotron can be built. However, present knowledge strongly implies that it can.

5.2. Injector cyclotron

A cyclotron could be used as injector to a synchrotron, since the latter requires injection energies of about, or less than, 10 MeV/n. However, the problems of properly matching a cyclotron to a synchrotron, especially as far as the time structure is concerned, have not been attacked and solved, yet, in a satisfactory way. This remains, however, an interesting possibility. In any case, if we limit ourselves to the consideration of fairly high charge states of light-medium weight ions, which is indeed the main goal of "MARIA", then the necessary K is more in the K=100 to 200 range. At these values it is quite doubtful that one should build a superconducting cyclotron, since the latter is really cost-effective with present day technology and know-how, only above the K 300-400 level.

6. Conclusions

The present analysis would lead to the conclusion that a superconducting cyclotron does not deserve further consideration, either as injector or as main machine, in view of nowadays "MARIA" requirements.

However, if for any reason whatsoever the desired energies will drop back to the earlier goals of ≃ 400 MeV/n or less, then the superconducting cyclotron can come back into the picture and probably represent a very viable and cost effective alternative.

References

1. H.G. Blosser, et al, MSUCL-222A(1976), unpublished.
H.G. Blosser; The Michigan State University Superconducting Cyclotron Program, IEEE Transactions on Nuclear Science, NS26 (1979) 2040.

2. F. Resmini, G. Bellomo, E. Fabrici, H.G. Blosser, D. Johnson; Design Characteristics of the K800 Superconducting Cyclotron at MSU, IEEE transactions on Nuclear Science, NS26 (1979) 2078.

3. K800 Conceptual Design Report; MSUCL-282 (December 1978).

4. G. Bellomo, F. Resmini; Trimming of the Magnetic Field for the K500 Cyclotron at MSU, MSUCP-31 (1980).

5. E. Fabrici, R.G. Resmini, A Survey of Beam Dynamics Prior to Extraction in the K500 Cyclotron at MSU, MSUCP-32 (1980).

6. E. Fabrici, D.Johnson, F.G. Resmini; The Extraction System for the K500 Cyclotron at MSU, MSUCP-33 (1980).

7. G. Bellomo, D. Johnson, P. Miller, F. Resmini; Magnetic Field Mapping of the K500 Cyclotron at MSU, MSUCP-30 (1980).

8. J.H. Ormrod et al., The Chalk River Superconducting Cyclotron, IEEE Trans. Nucl. Sci. NS-26 (1979) 2034.

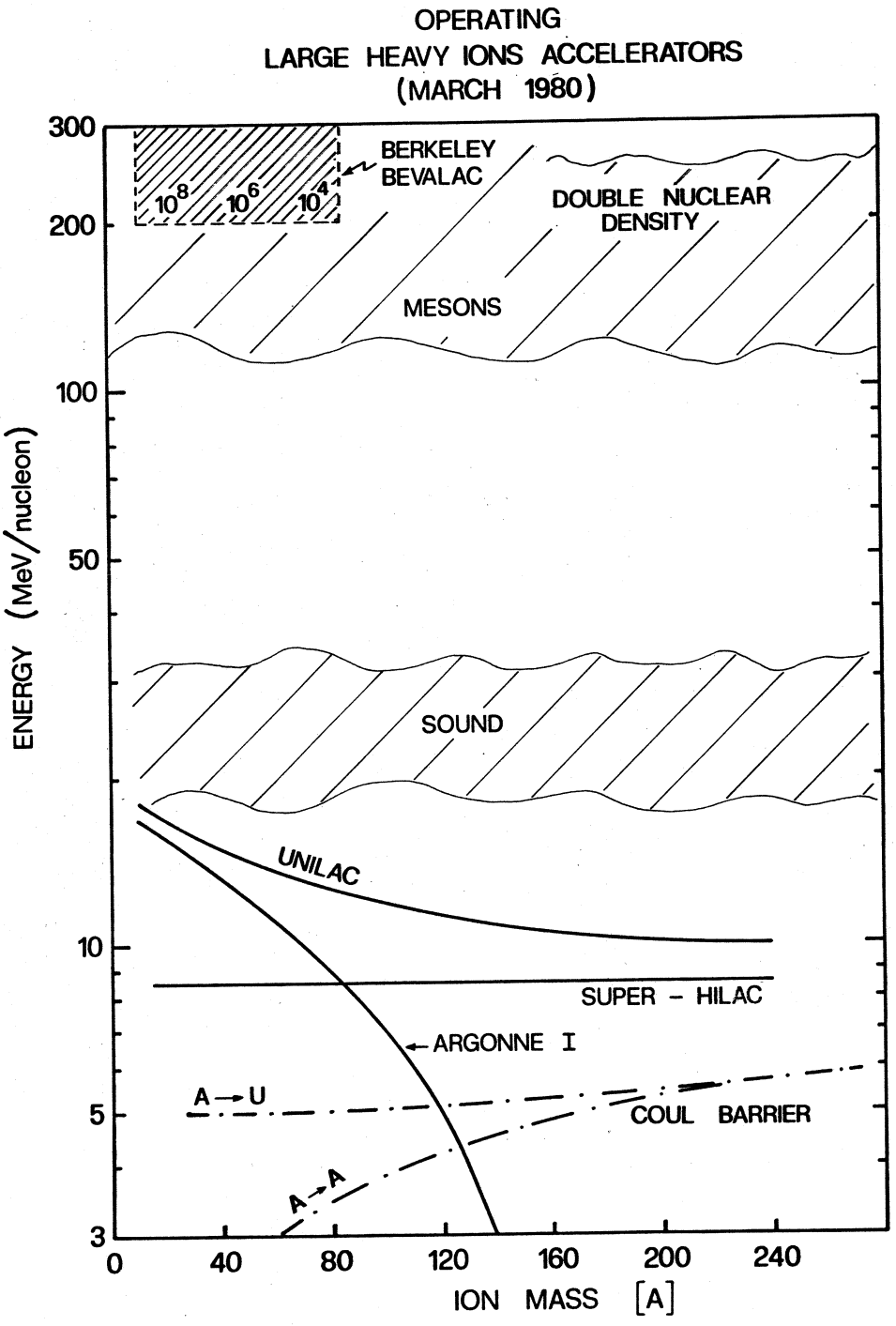

Fig. 1. Energy vs A diagrams of major heavy ion facilities now in operation.

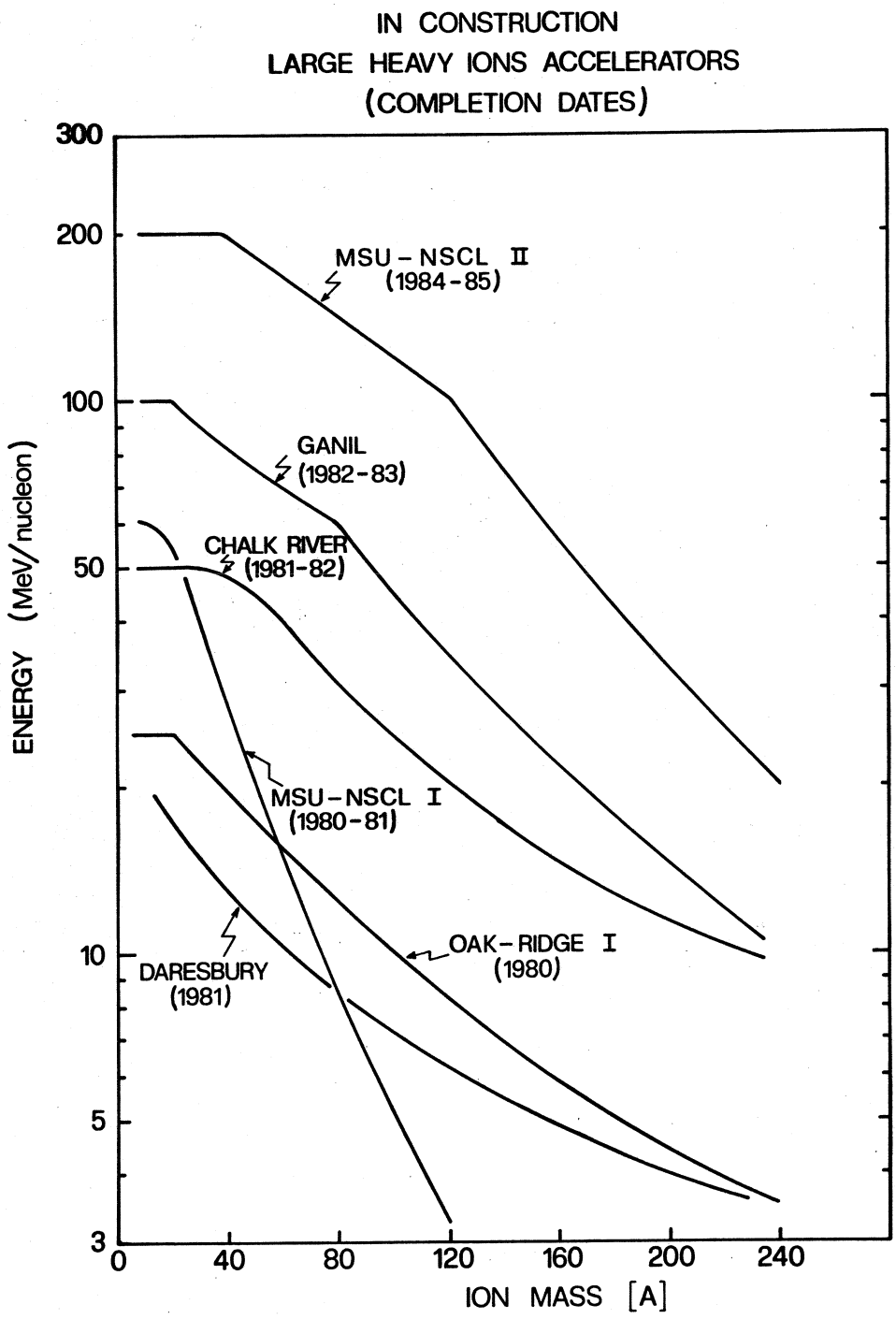

Fig. 2. Large heavy ion accelerators presently under construction.

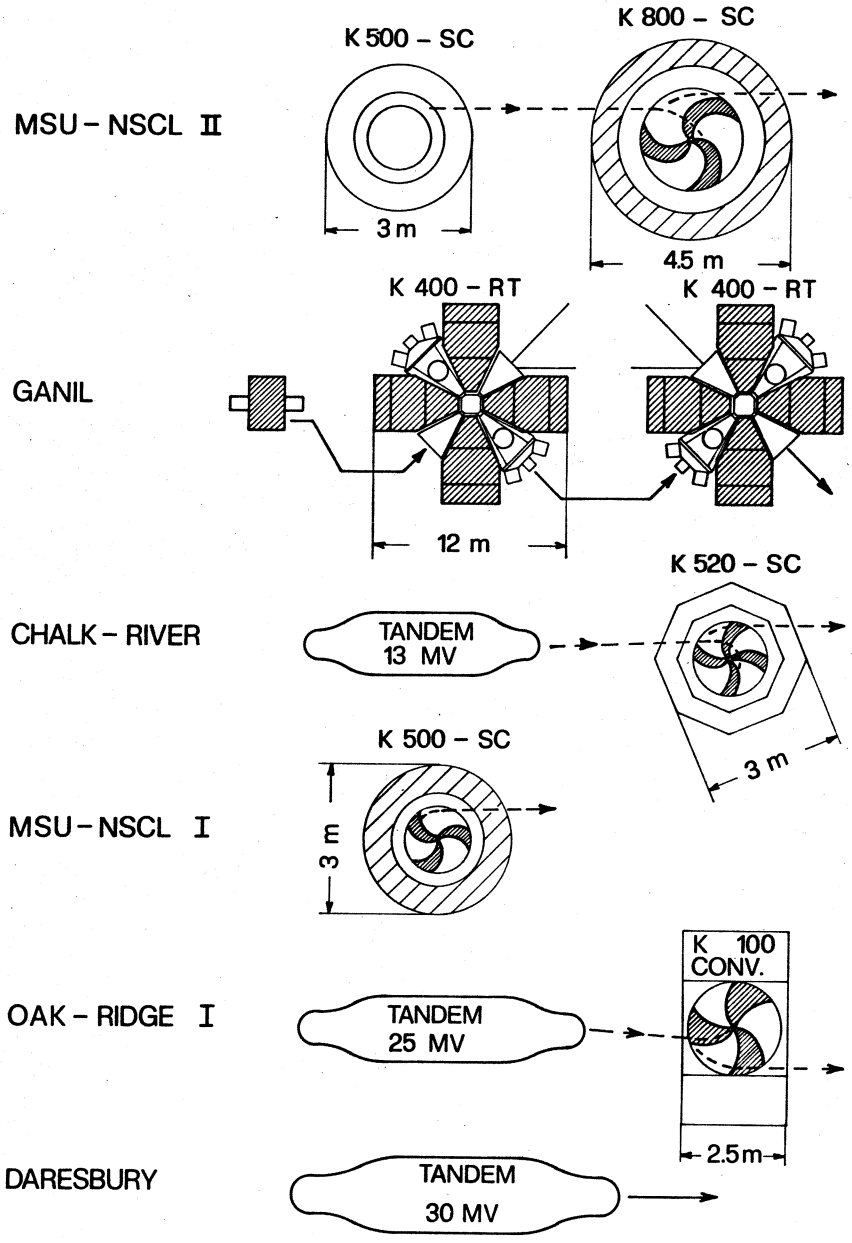

Fig. 3. Schemes of presently built accelerators.

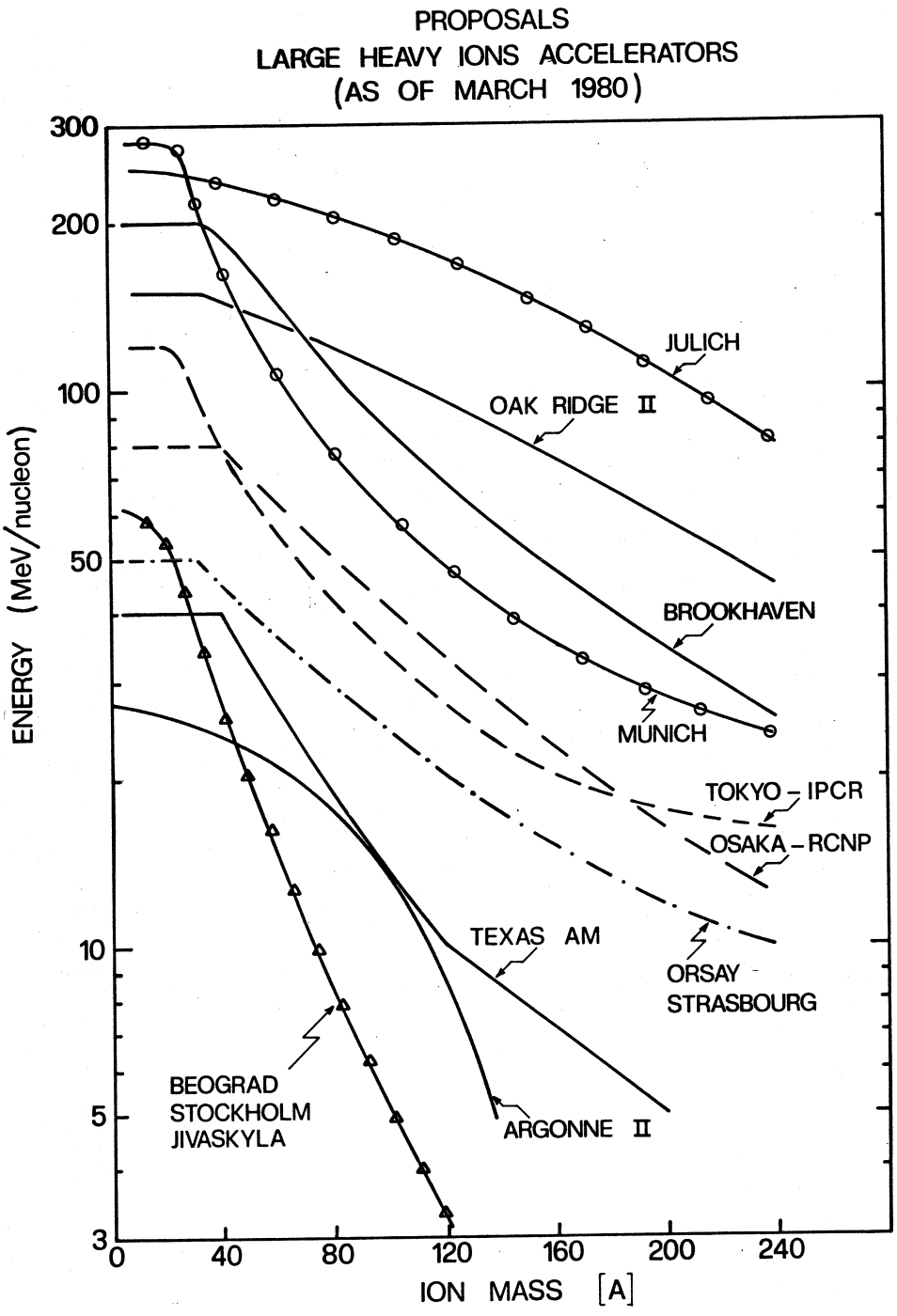

Fig. 4. New proposals for heavy ion accelerators in the 30 to 300 MeV/n range.

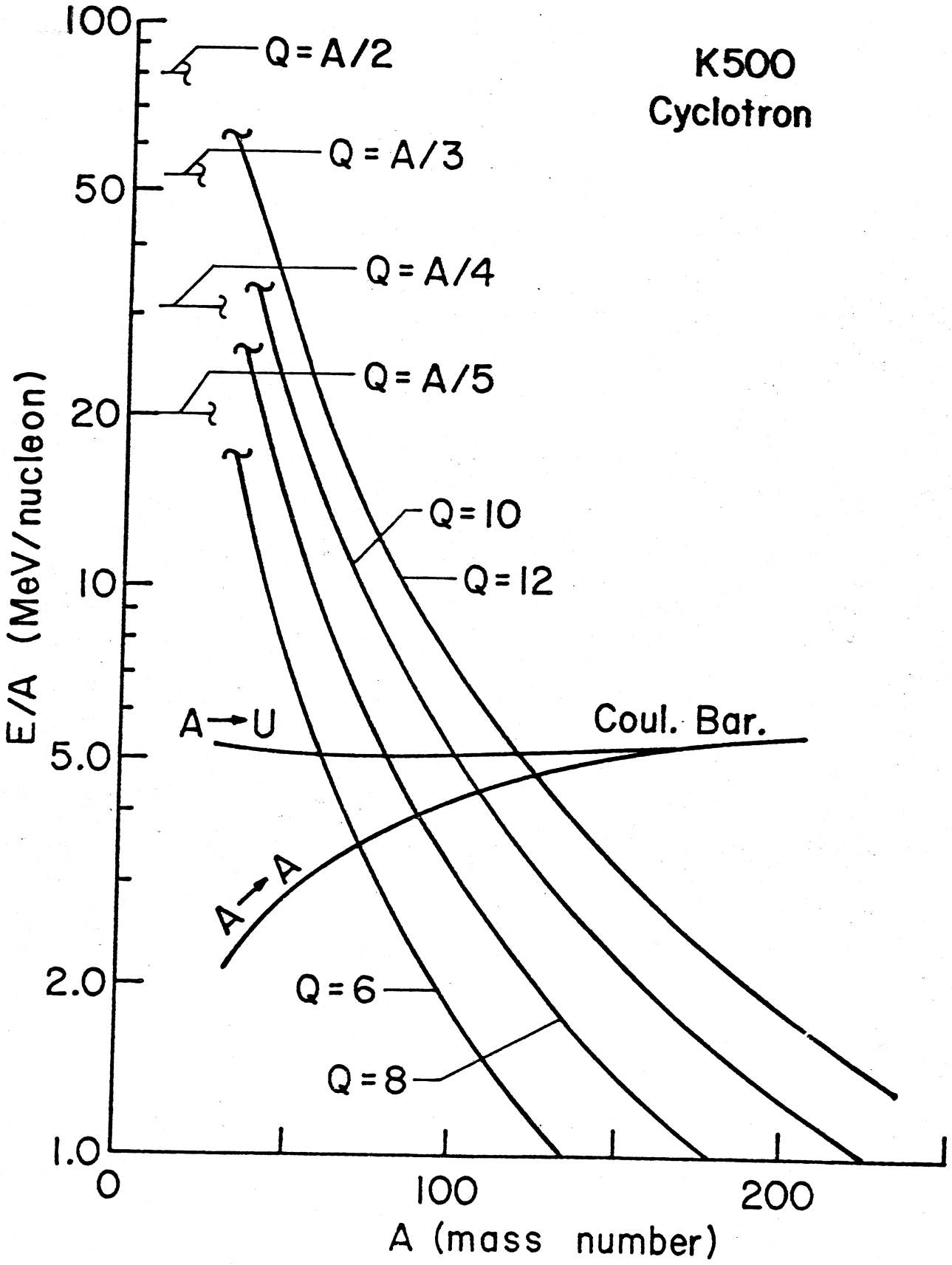

Fig. 5. T/A vs A for the K=500 cyclotron lines of constant change state delivered by an internal ion source are shown.

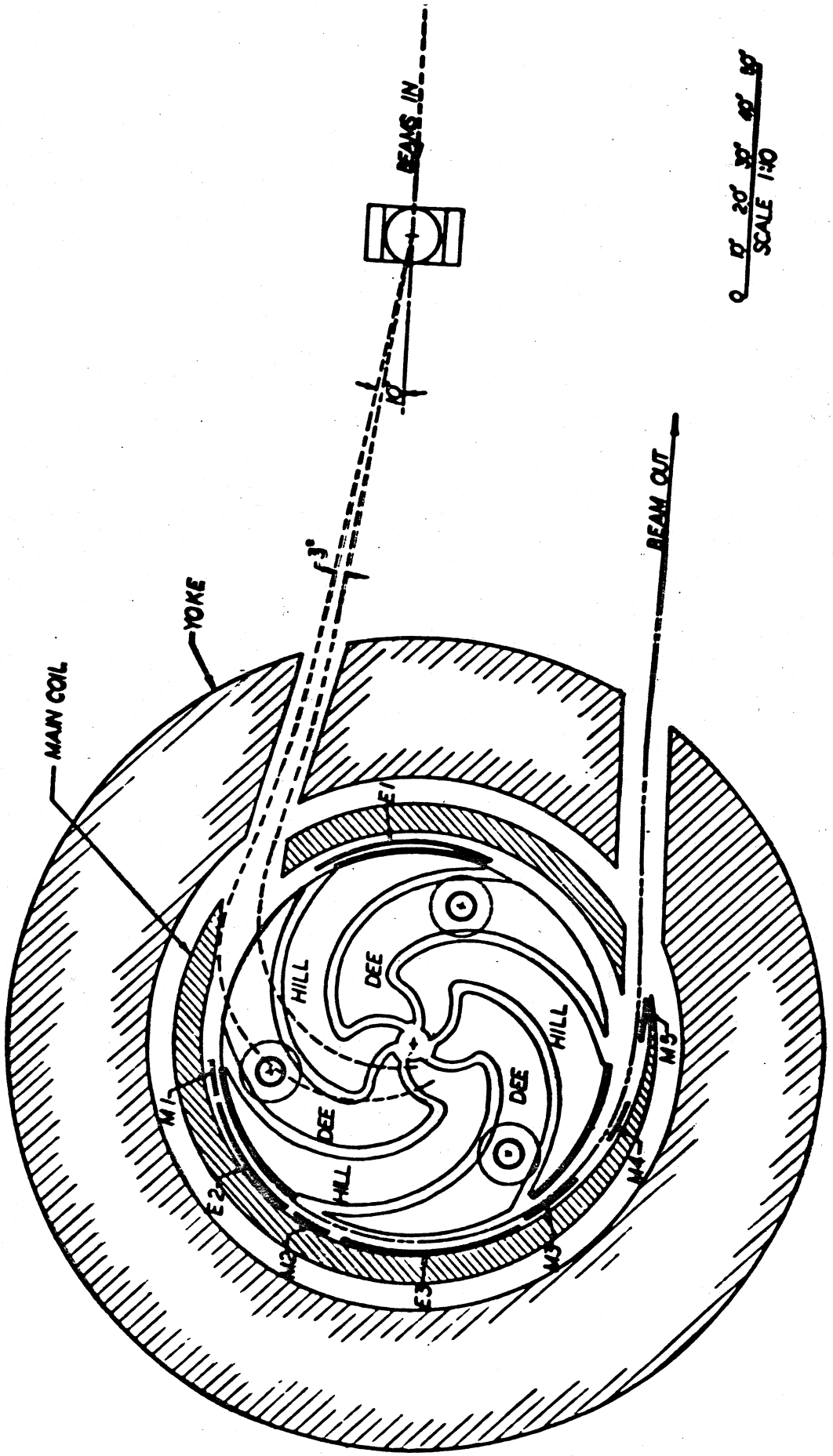

Fig. 6. Injection scheme of beams from the K500 cyclotron into the K800 cyclotron.

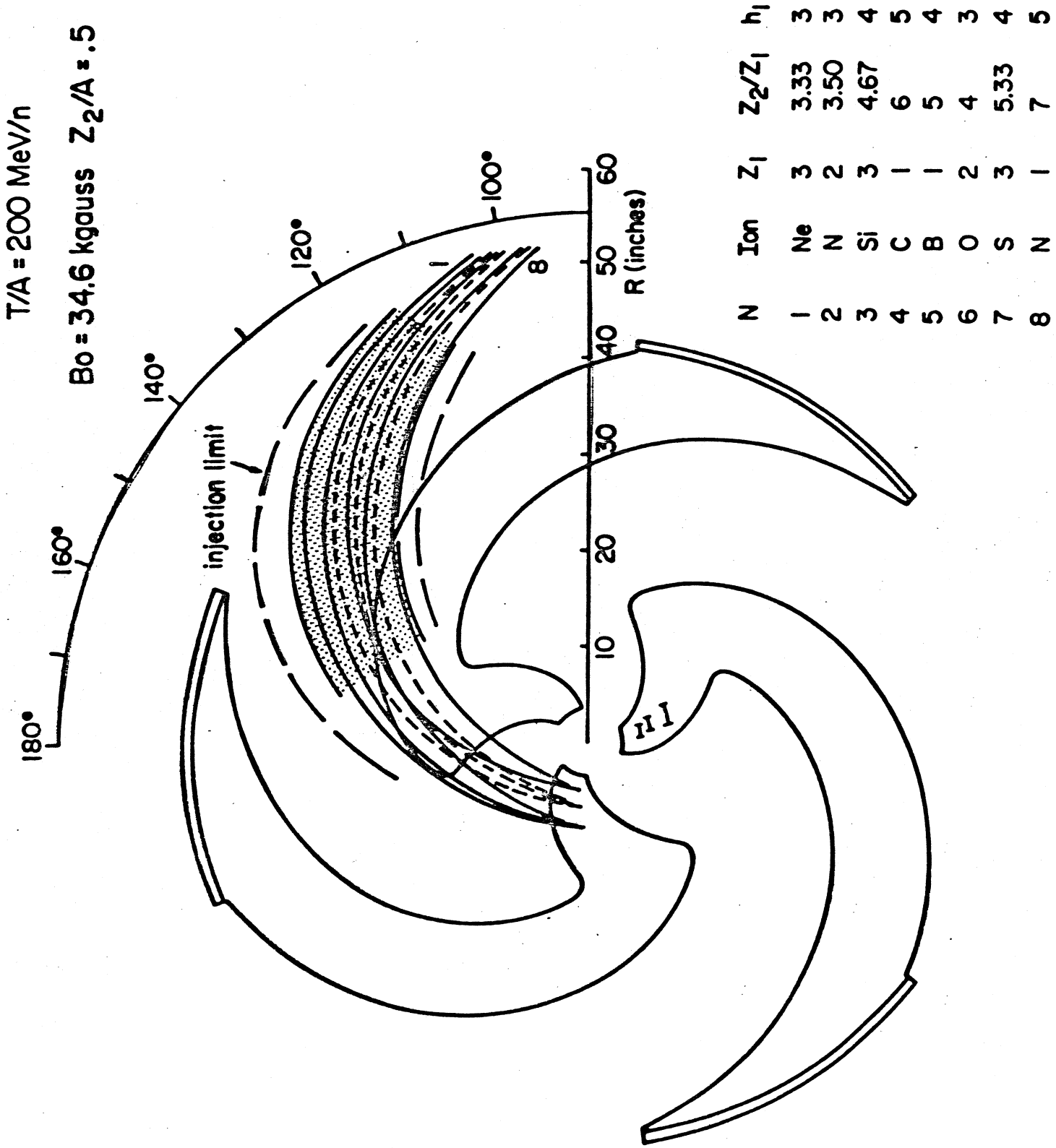

Fig. 7. Injection trajectories and stripping portions for light ions (final energy 200 MeV/n) in the K800 cyclotron.

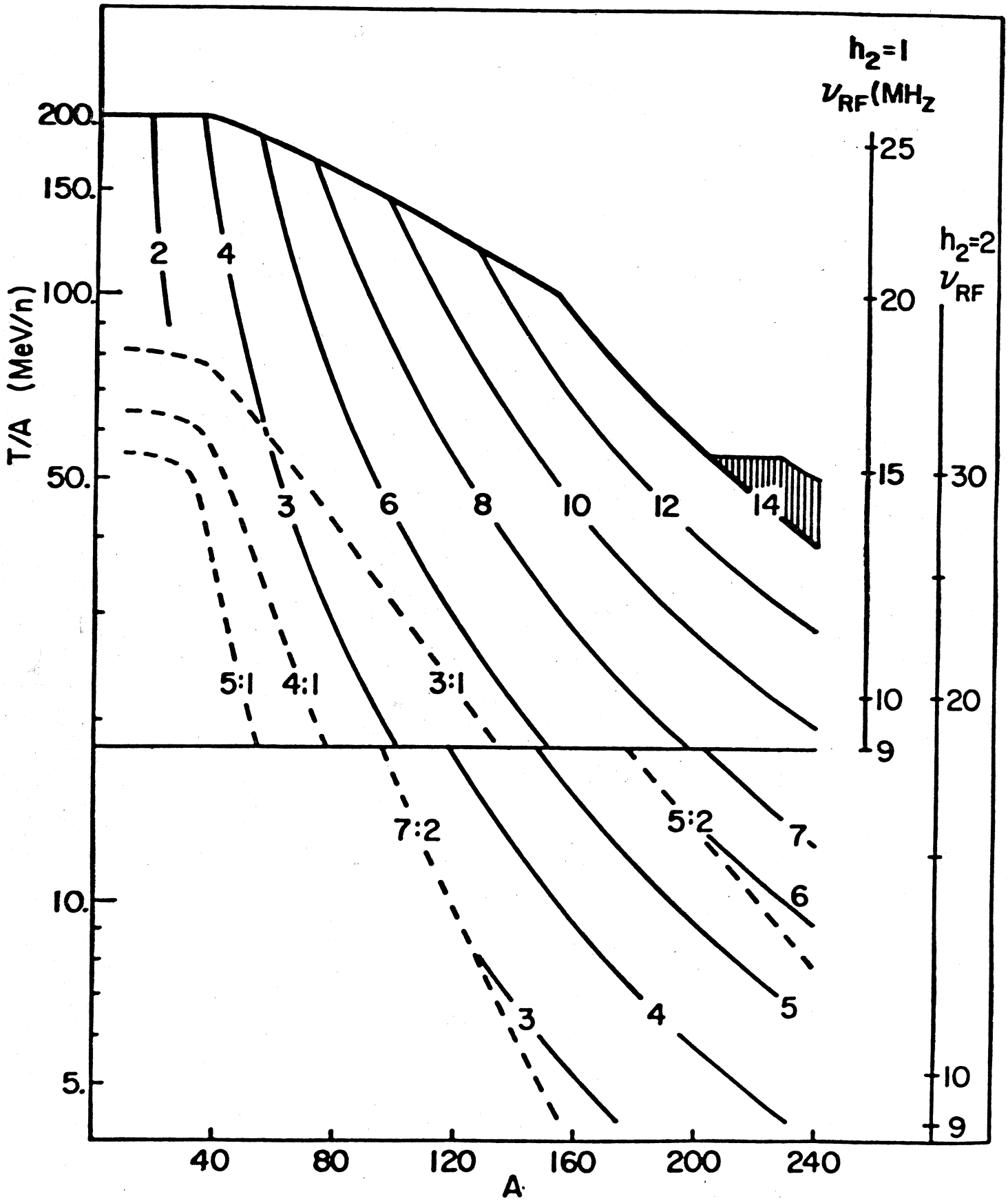

Fig. 8. T/A va A for the K800 cyclotron. Lines of constant charge state from the K500 cyclotron are shown.

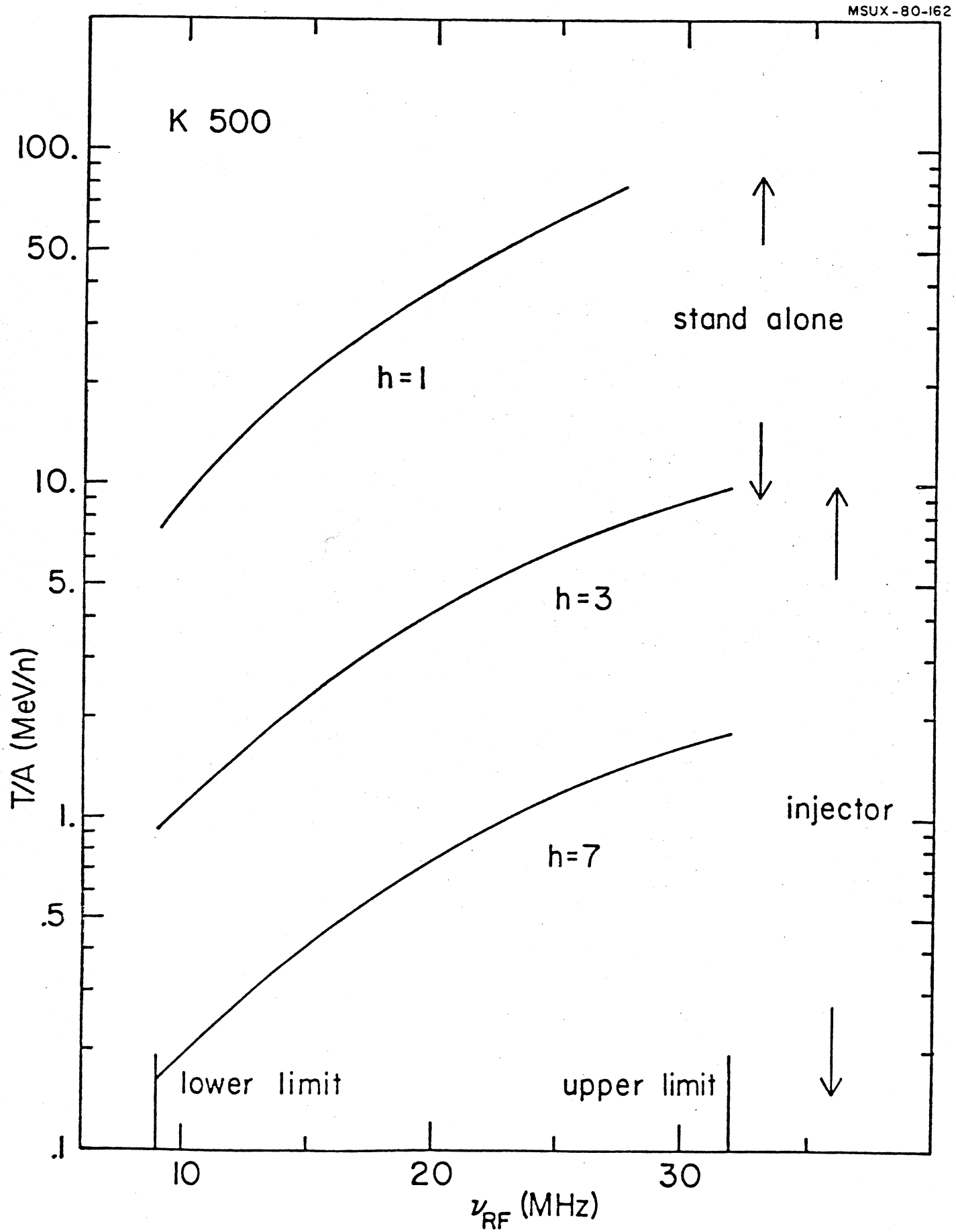

Fig. 9. Acceleration frequency vs ion energy for the K500 cyclotron, for several harmonic modes.

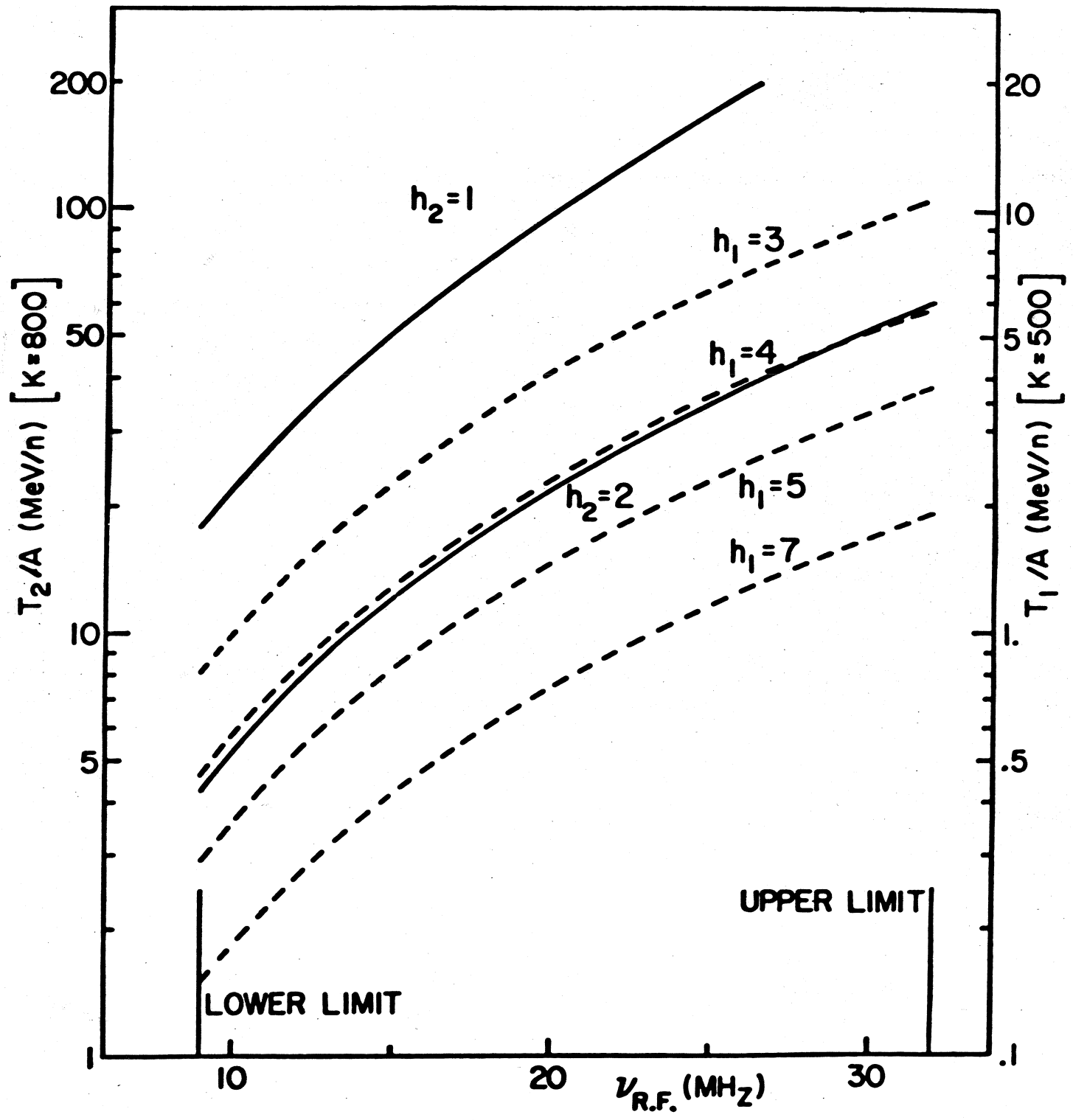

Fig. 10. Acceleration frequency vs ion energy for the coupled $K800_2$ and $K500_1$ cyclotrons showing the different harmonic modes used in the two machines.

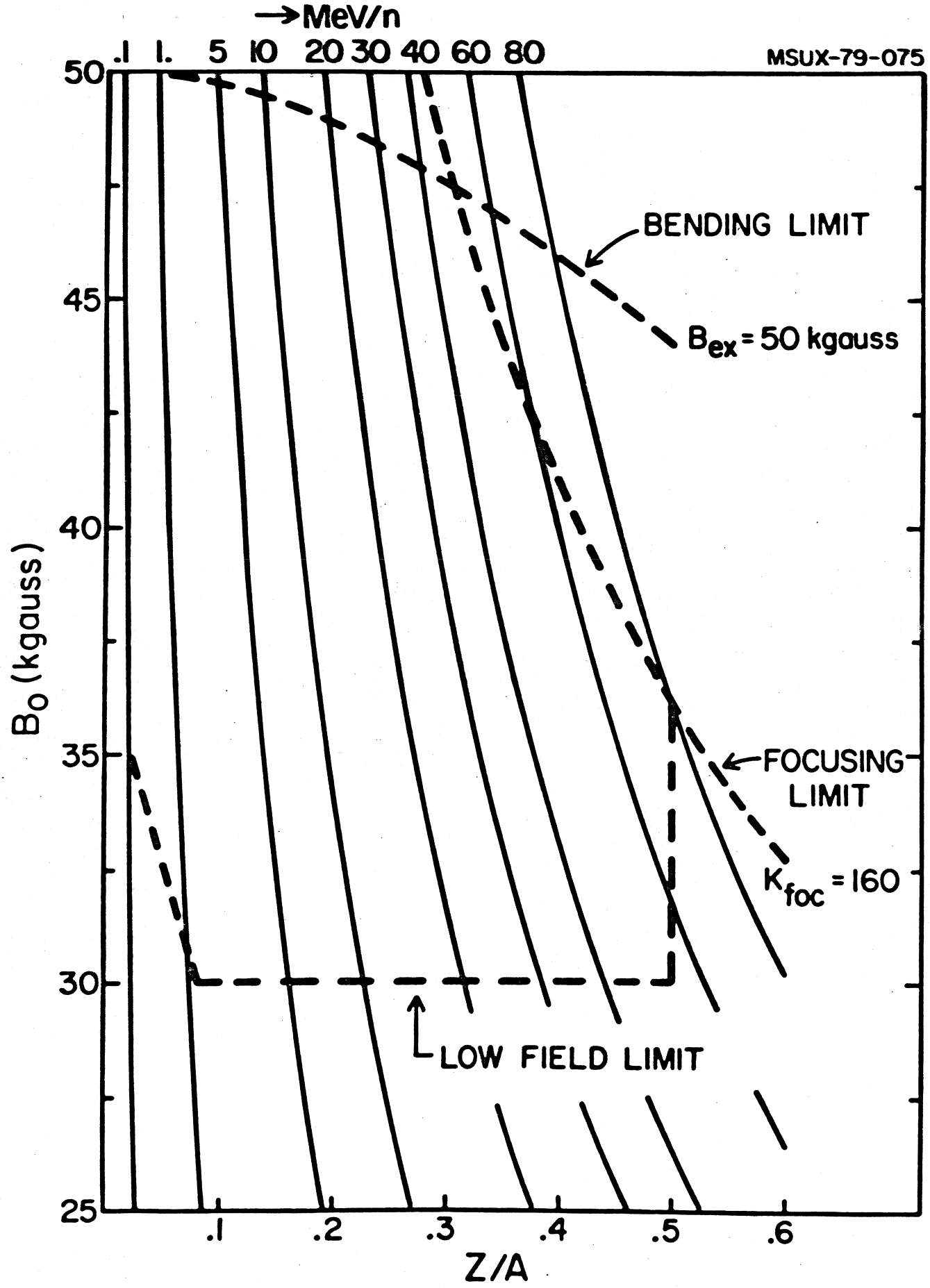

Fig. 11. Operating diagram of the K500 cyclotron in the (B_o, Z/A) plane. Constant energy/nucleon lines are shown.

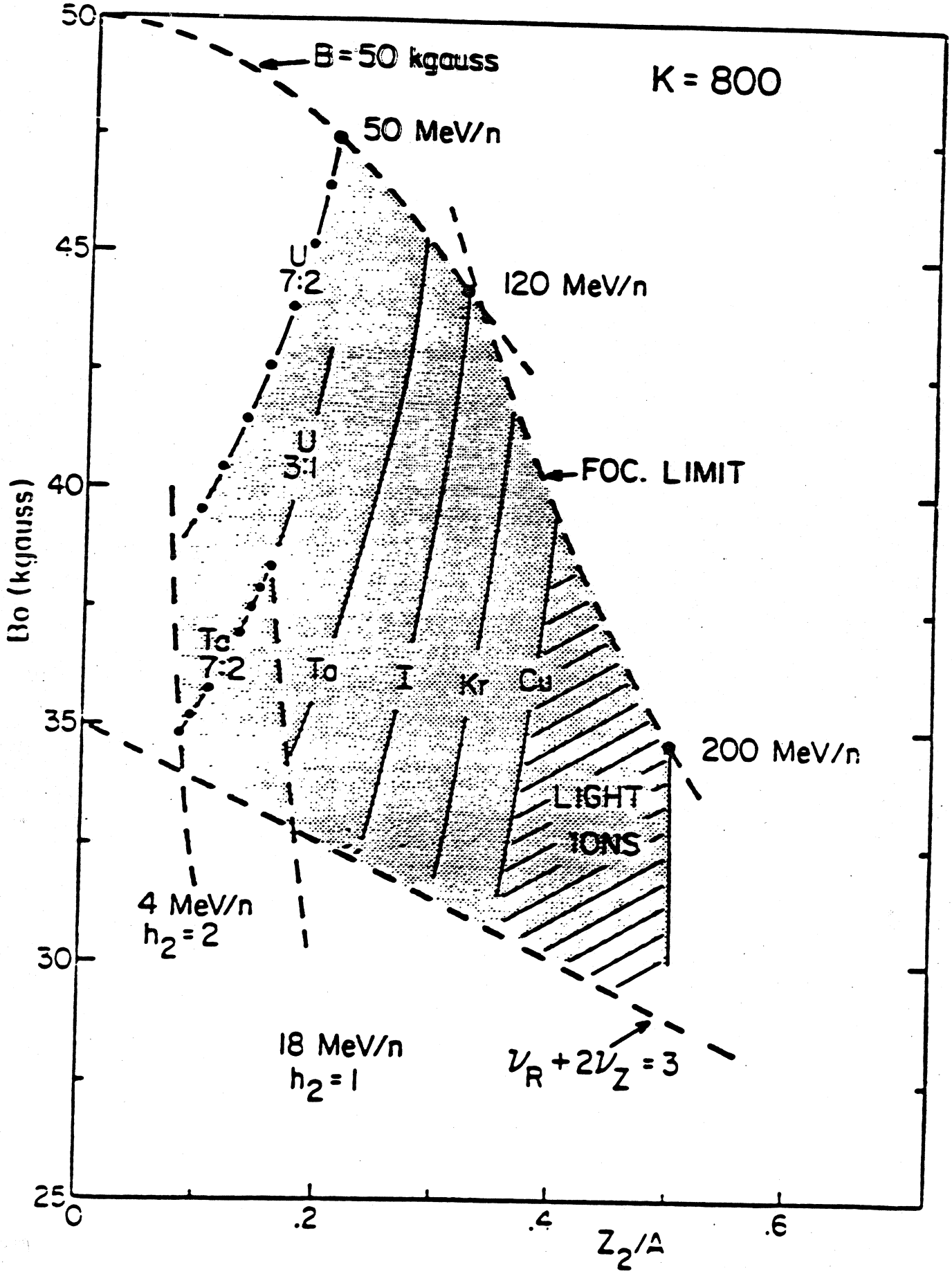

Fig. 12. Operating diagram of the K800 cyclotron in the (B_o, Z/A) plane.

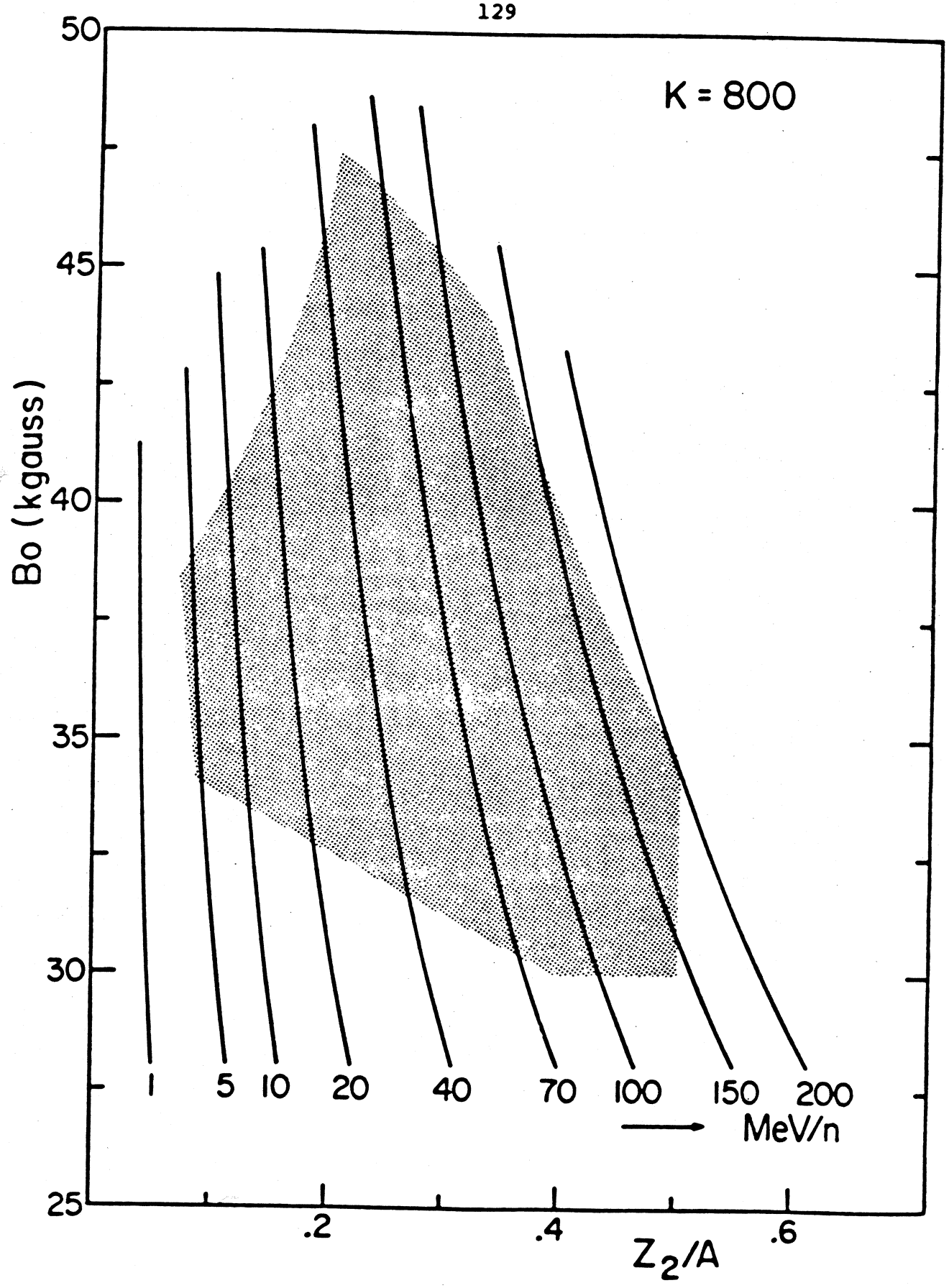

Fig. 13. Constant energy/nucleon lines, for the K800 cyclotron across its operating diagram in the (B_0,Z/A) plane.

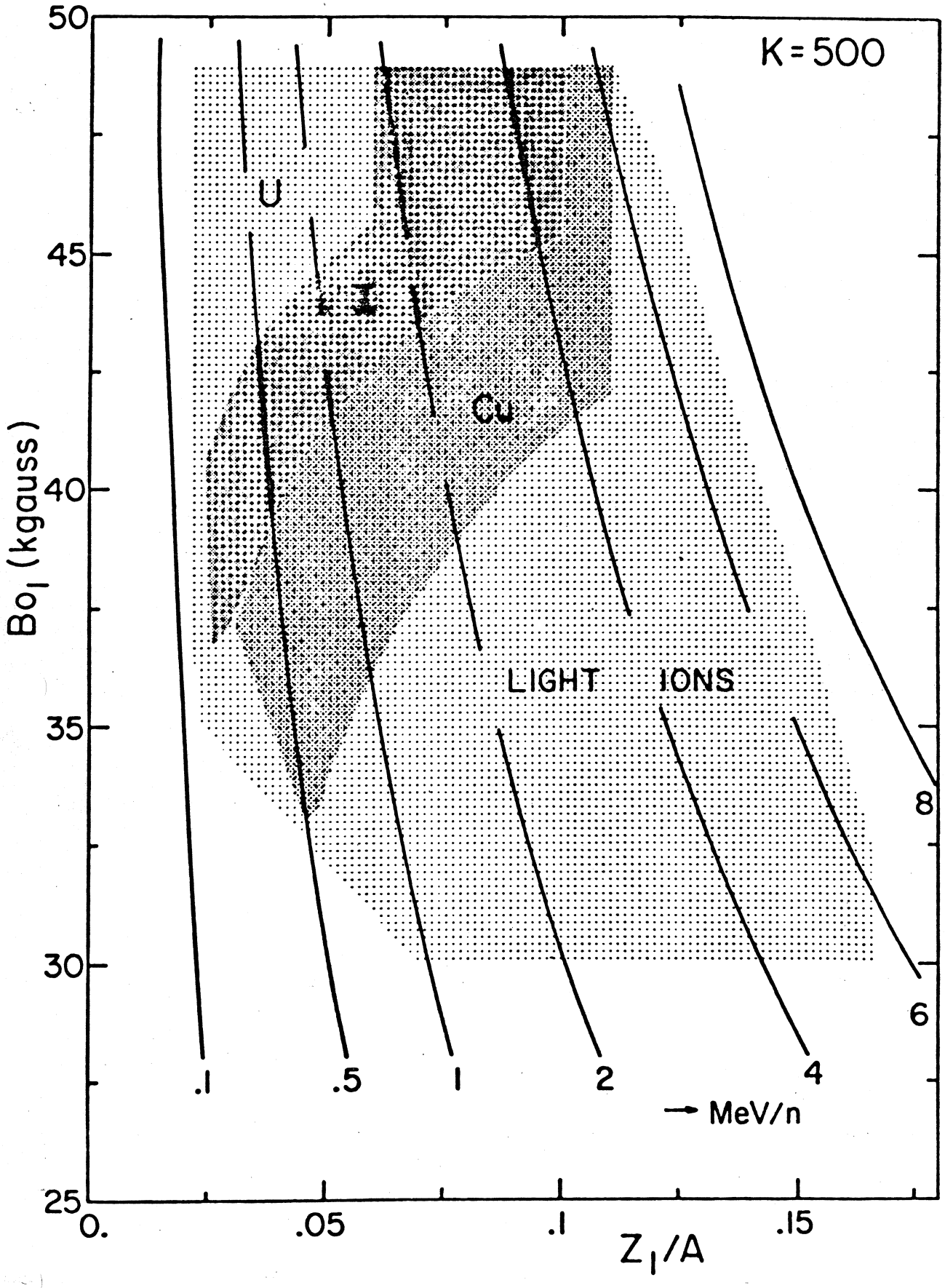

Fig. 14. Operating diagram of the K500 cyclotron in the (B_o,Z/A) plane when acting as injector. Constant energy/nucleon lines are shown.

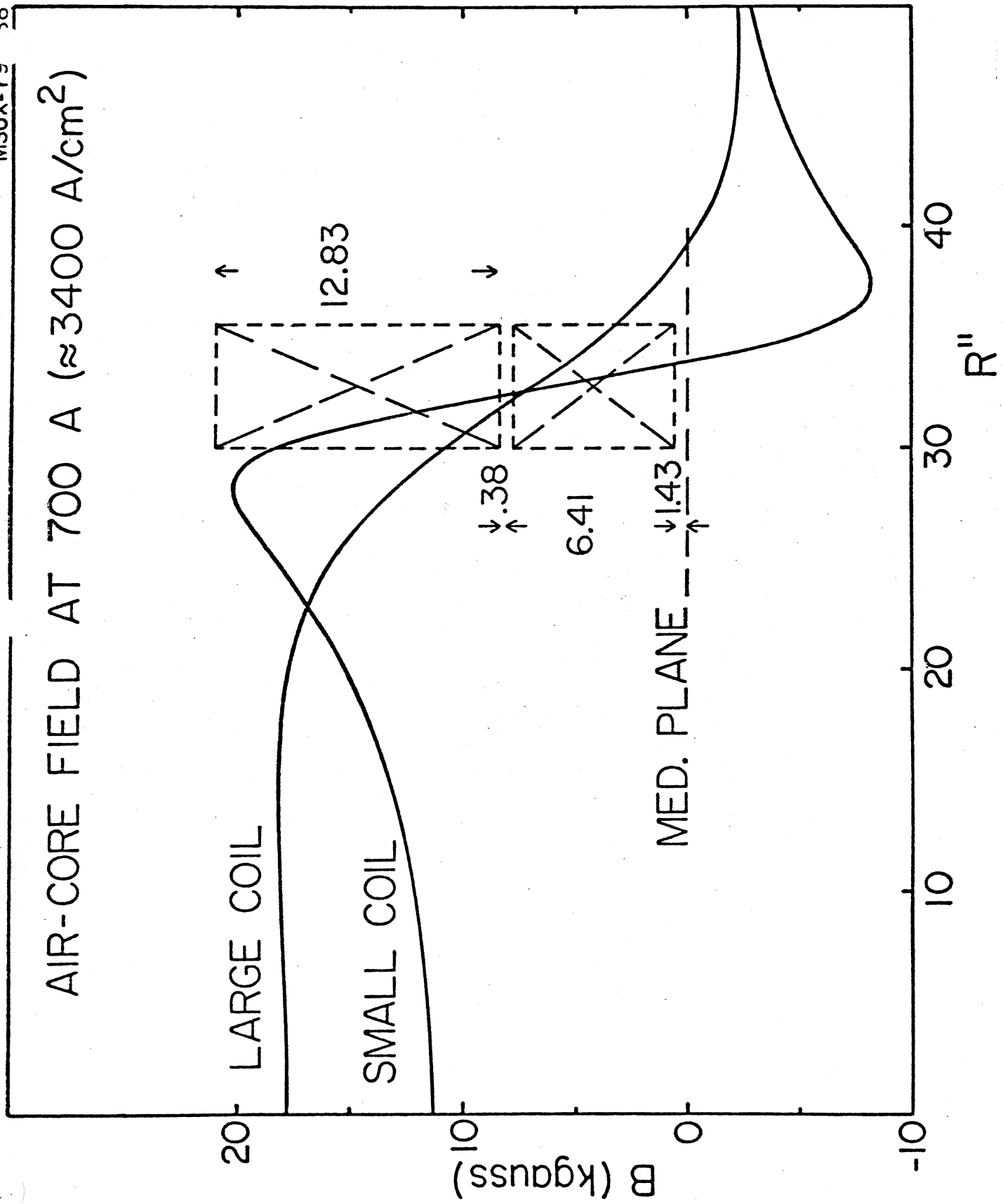

Fig. 15. Air core fields of the two sections of the K500 coils, at maximum excitation.

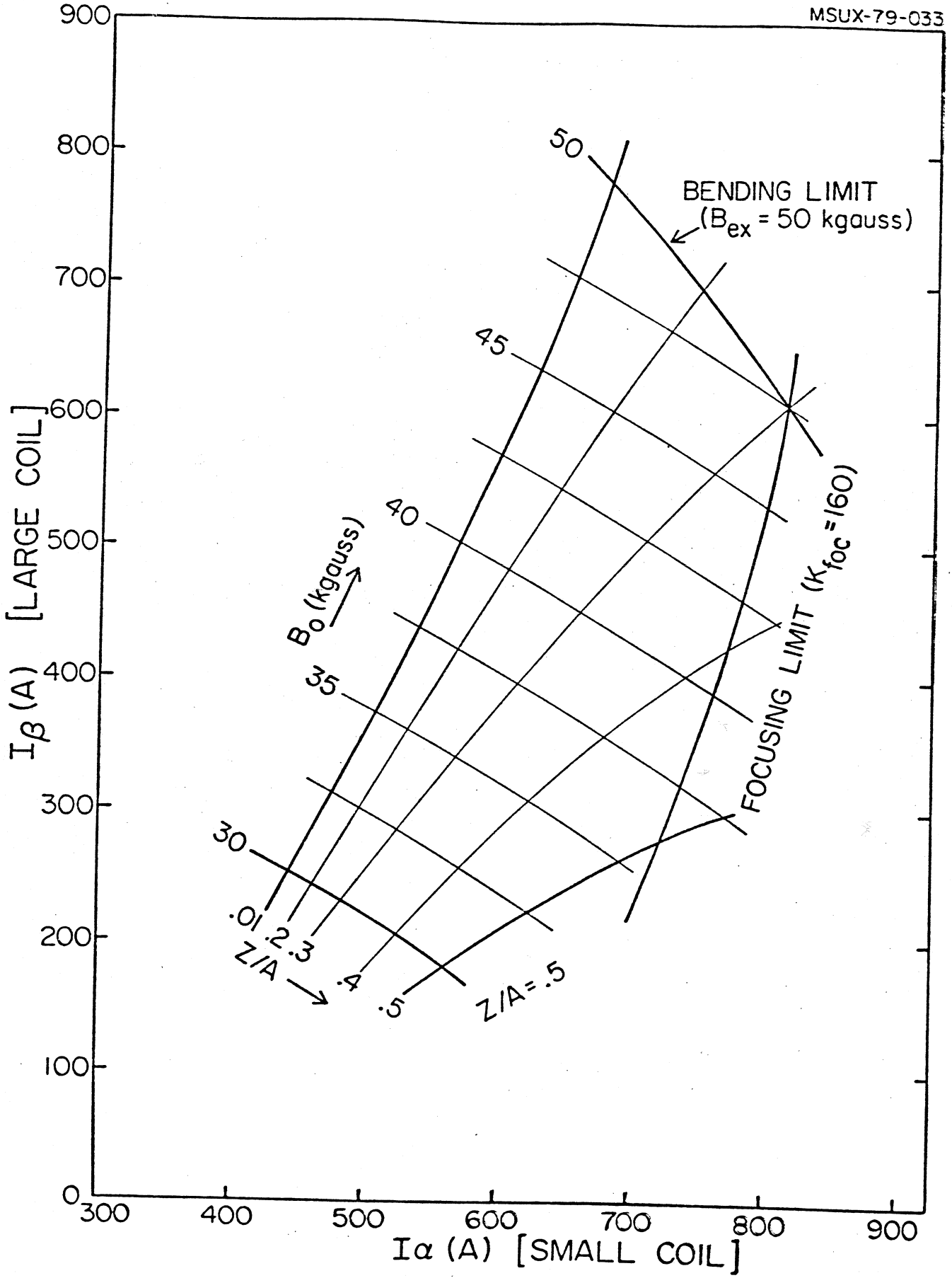

Fig. 16. Operating diagram of the K500 cyclotron in the space of the excitation currents of the two main coil sections. Lines of constant Z/A and B_o are shown, together with focusing and bending limits.

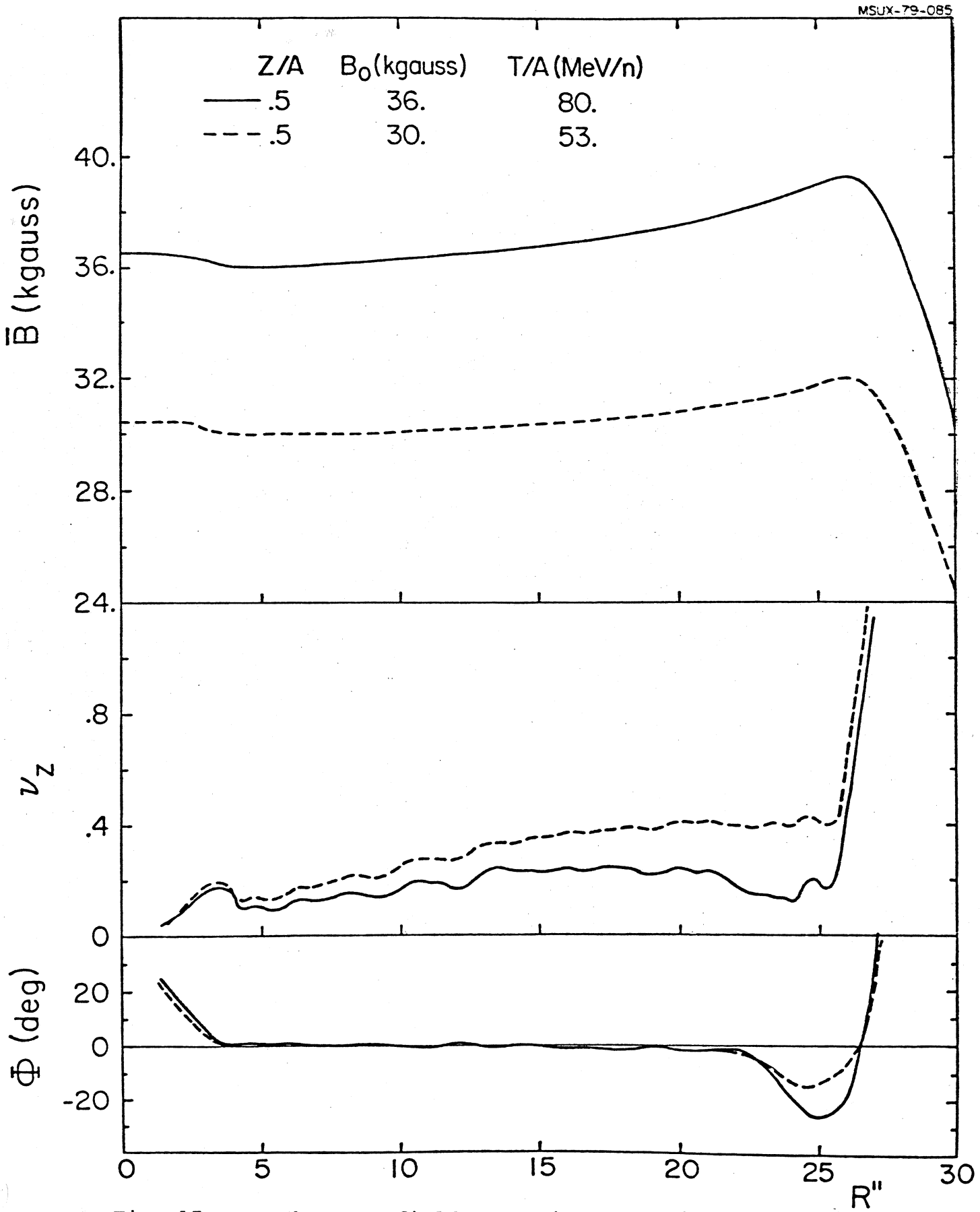

Fig. 17. Isochronous fields, vertical focusing frequencies and accelerating phase of Z/A = .5 ions, with different final energies, in the K500 cyclotron.

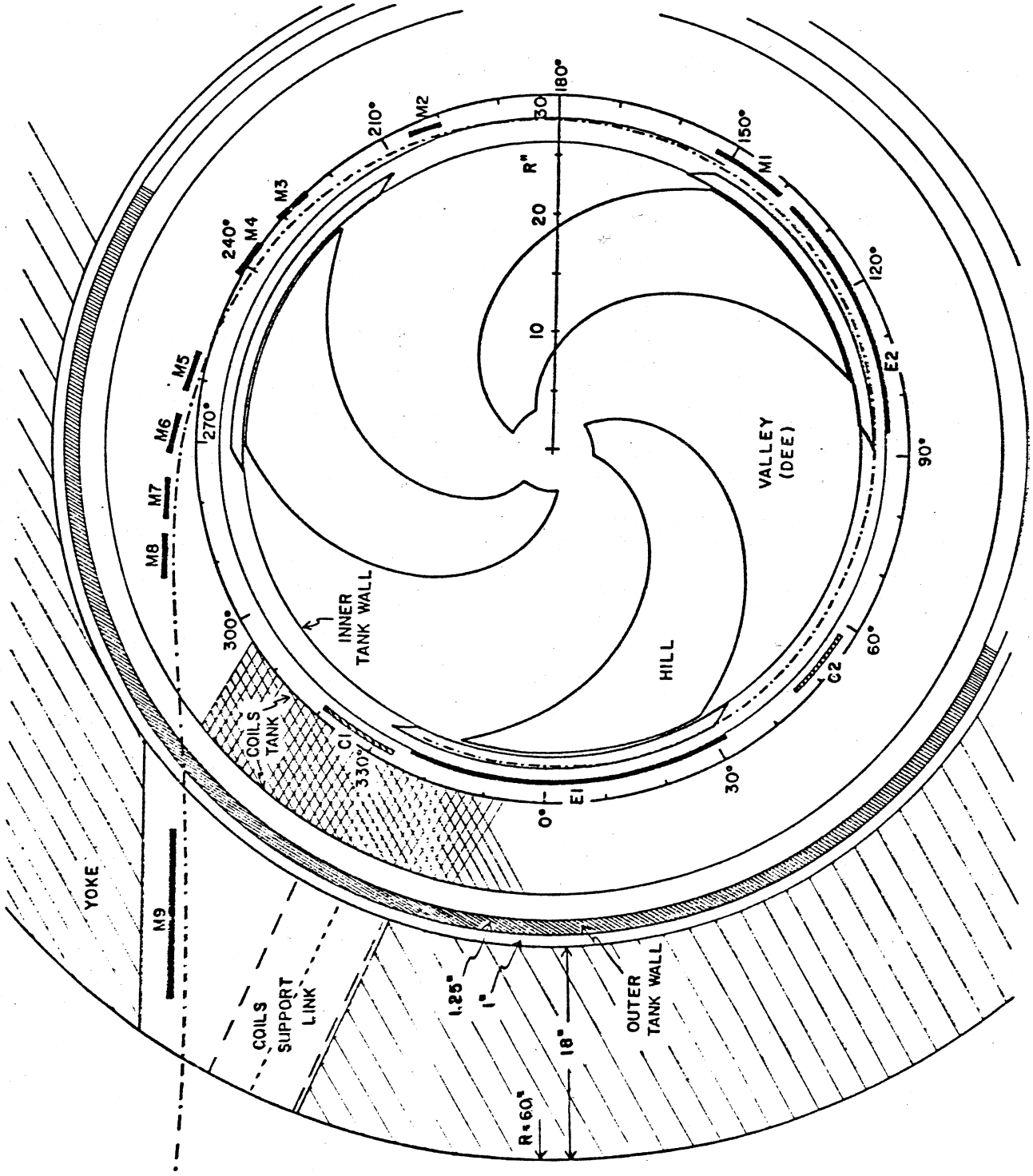

Fig. 18. Extraction scheme for the K500 cyclotron. E_1 and E_2 are electrostatic deflectors, while M_1 to M_9 are magnetic channels of the passive type as shown in Fig. 19.

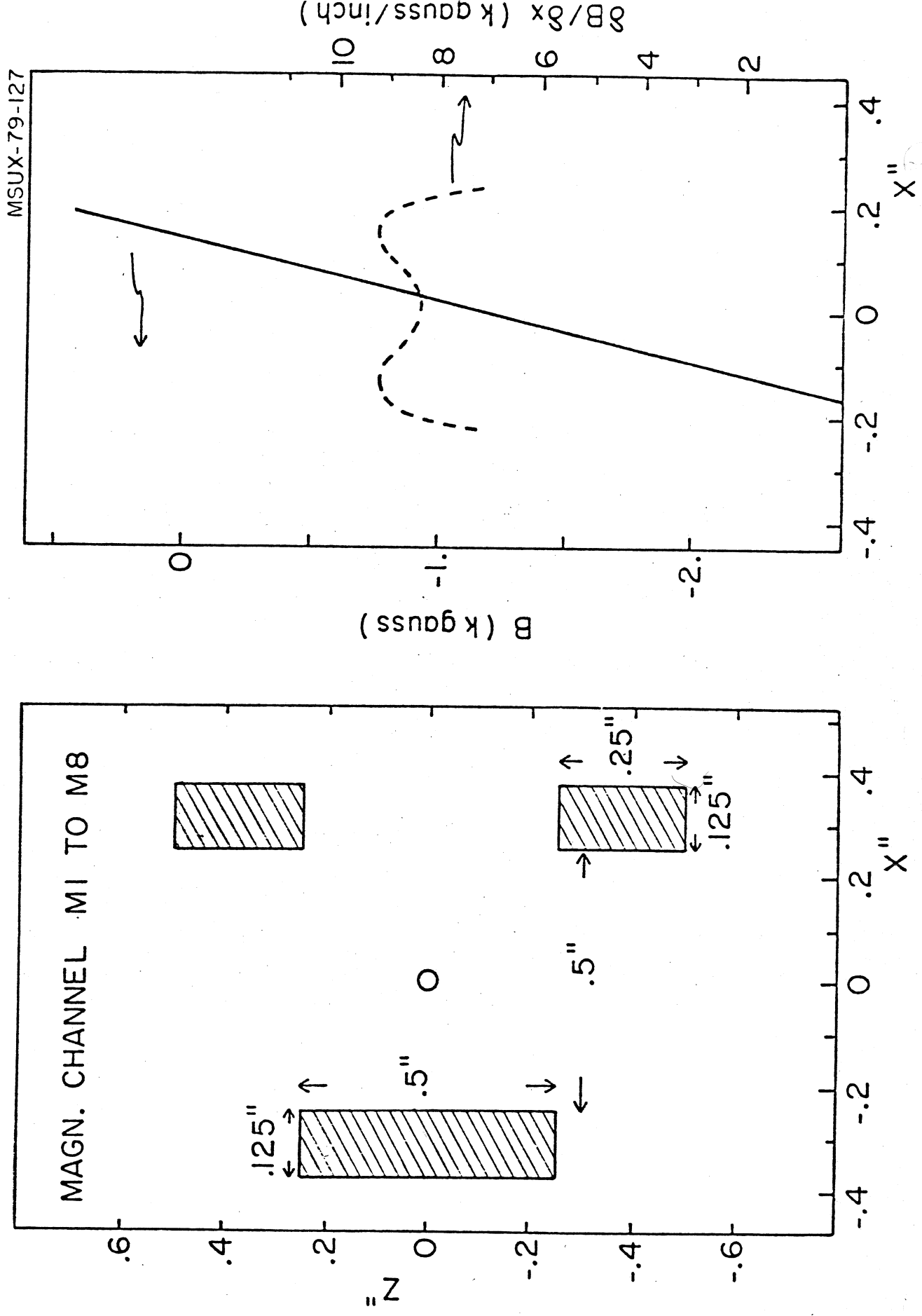

Fig. 19. Cross section of a typical passive magnetic channel used in the K500 cyclotron extraction scheme. Field gradients thus obtained are shown at left.